Article

Not peer-reviewed version

Pedestrian-Level Cooling Performance Index and Climate-Adaptive Layout of Tropical Commercial Plots Under Constant Development Intensity

Yilin Cen , Jiacheng Jiao * , Dawei Mu , Yuwei Wu , Yang Yang , Fashu Yi , Xintong Liu , Feilin Zheng , Jun Hu *

Posted Date: 15 May 2026

doi: 10.20944/preprints202605.1065.v1

Keywords: commercial plots; building layout; wind environment; cooling performance; pedestrian level

 doi:10.20944/preprints202605.1065.v1

Article

Pedestrian-Level Cooling Performance Index and Climate-Adaptive Layout of Tropical Commercial Plots Under Constant Development Intensity

Yilin Cen [1], Jiacheng Jiao [1,*], Dawei Mu [1], Yuwei Wu [1], Yang Yang [2], Fashu Yi [1], Xintong Liu [3], Feilin Zheng [4] and Jun Hu [1,5,6,*]

[1] School of Civil Engineering and Architecture, Hainan University, Haikou 570228, China
[2] School of Qilu Transportation, Shandong University, Jinan 250061, China
[3] Manchester School of Architecture, Manchester Metropolitan University, Manchester M15 6BR, United Kingdom
[4] HNU-ASU International College, Hainan University，Haikou 570110, China
[5] State Key Laboratory of Tropic Ocean Engineering Materials and Materials Evaluation, Hainan University, Haikou 570228, China
[6] Collaborative Innovation Center of Marine Science and Technology, Hainan University, Haikou 570228, China
* Correspondence: Jiaojiac1993@163.com (J.J.); hj7140477@hainanu.edu.c (J.H.)

Abstract

In tropical island cities, the combined pressures of rapid high-density urbanization and year-round hot-humid climates make the pedestrian-level wind environment a critical determinant of outdoor thermal comfort and cooling performance. Focusing on Haikou, a tropical island city, this study optimizes building layouts on commercial plots under constant development intensity. A Pedestrian-level Cooling Performance Index (PLCPI) was constructed, prioritizing summer cooling and winter wind control through an AHP-EWM combined weighting method. The index integrates maximum pedestrian-level wind speeds and amplification factors to evaluate 65 layout configurations, including detached, row, perimeter, and courtyard types. The results reveal a nonlinear relationship between building count and cooling performance. Single-building layouts achieve the highest mean PLCPI (2.367), three-building layouts the lowest (1.825), prone to ventilation stagnation, and four-building layouts show a performance rebound (2.271) with stable efficiency. Crucially, spatial enclosure form is the decisive determinant under a constant building count: the optimal two-building layout B-8 (PLCPI=2.456) surpasses the best single-building layout A-2 (2.419), demonstrating that well-designed dispersed layouts can outperform centralized ones. This study proposes a dual-season adaptive evaluation framework for tropical commercial plots and reveals the nonlinear mechanism between building quantity and cooling performance, providing a scientific basis for fine-grained urban design in tropical island climates.

Keywords: commercial plots; building layout; wind environment; cooling performance; pedestrian level

1. Introduction

With the acceleration of global urbanization, high-density urban development has brought about economic agglomeration effects while simultaneously triggering numerous environmental concerns. Wind, a critical natural element governing urban microclimates, plays a pivotal role in pollutant dispersion, thermal comfort regulation, and ultimately, public health and the functional quality of urban spaces [1]. Current scholarship has investigated this subject from multiple dimensions, with research trajectories primarily categorized into three areas: the interplay between

 doi:10.20944/preprints202605.1065.v1

wind environment and building layout, its role in thermal mitigation, and its impact on pedestrian-level comfort.

Early explorations into the wind environment–building layout nexus primarily employed wind tunnel experiments, focusing on the aerodynamic effects of isolated building forms. Stathopoulos (1985) demonstrated through wind tunnel tests that corner-cut designs in high-rise buildings can significantly reduce the area of high-wind zones at ground level, with this effect becoming more pronounced as building height increases [2]. The advent of computational fluid dynamics (CFD) in the 21st century shifted the focus toward simulations of complex building clusters. Hu and Wang (2005) observed that while CFD simulations align well with wind tunnel results under conditions of regular layouts and uniform heights, predictive accuracy diminishes with significant height variations, underscoring the methodological challenges posed by complex urban morphologies [3]. Using Large Eddy Simulation (LES), Aristodemou et al. (2018) revealed that high-rise clusters in London drastically alter surrounding airflow structures, creating pollutant concentration zones with limited dispersion [4]. Extending the analysis to the vertical dimension, Lu et al. (2022) found that building height distribution patterns significantly affect vertical wind speed and pressure, indicating that uniform-height layouts are more conducive to overall wind comfort [5]. From a design perspective, Guo et al. (2022) compared Chinese Feng Shui layouts with modified layouts at Prince Kung's Palace in Beijing, validating that nature-responsive building arrangements significantly optimize courtyard ventilation during summer [6]. Furthermore, Zhao et al. (2023) investigated non-enclosed atrium spaces, uncovering how indoor morphology influences airflow penetration and temperature distribution [7]. Collectively, these studies trace an evolution from static analyses of solitary forms to systematic, dynamic investigations of complex urban fabrics and their vertical ventilation effects. Nevertheless, a significant lacuna remains in the literature: the characterization of wind environments across different land-use types and a systematic consideration of urban adaptation strategies for tropical regions.

The link between the wind environment, urban cooling, and the heat island effect is a core issue of sustained academic interest. At the macro-scale, Ngarambe et al. (2021), based on nine years of meteorological observation data from Seoul, quantitatively revealed the significant impact of wind speed on urban heat island intensity, finding that increased wind speeds lead to a decrease in intensity, which is notably higher in dense building areas than in sparse ones [8]. At the micro-scale, Davtalab et al. (2020) demonstrated in the context of Iran that areas with vegetation cover exhibit significant reductions in air temperature, mean radiant temperature, and physiological equivalent temperature compared to non-vegetated areas, indicating complex interactions between wind, vegetation, and the underlying surface [9]. Research by Chan and Chau (2021) on urban parks in Hong Kong further revealed pronounced seasonal variations in this relationship; factors such as surrounding building layout and park size were found to be more critical for thermal comfort in summer, while building spacing played a more significant role in winter [10]. Similarly, Deng and Wong (2020) systematically analyzed the impact of street aspect ratios and orientations on outdoor thermal comfort through simulations of street canyon scenarios in Nanjing's central business district, discovering a significant correlation between canyon geometry and physiological equivalent temperature [11]. At a broader urban scale,Yang et al. (2020) and Zeng et al. (2024) utilized multi-source remote sensing data and the Local Climate Zone (LCZ) framework, respectively, to verify the positive correlation between building morphology and heat island intensity from a broader perspective of urban form [12,13]. These studies collectively indicate that research on wind environments and urban cooling effects has advanced from macro-scale meteorological statistics to micro-scale local climate regulation, with an increasing focus on multi-factor coupling mechanisms. However, most existing studies focus on single-season or macro-scale analyses. Consequently, there is a dearth of empirical evidence to guide layout optimization that simultaneously addresses the dual objectives of summer cooling and winter wind control.

Pedestrian-level wind comfort is of paramount importance, as it is directly intertwined with the usability of urban public spaces. Kubota et al. (2008) conducted wind tunnel experiments across 22

 doi:10.20944/preprints202605.1065.v1

residential neighborhoods in Japan, revealing a robust correlation between the building coverage ratio and the mean wind speed ratio at the pedestrian level [14]. Li et al. (2012) corroborated this in the context of South China, finding that a increase in building coverage leads to a linear decrease of 0.1 in the wind speed ratio [15]. As the field advanced, Iqbal and Chan (2016) examined the effects of spacing, orientation, and wind incidence angles within cruciform high-rise clusters, discovering that vortices formed under oblique winds can paradoxically enhance wind comfort [16]. Furthermore, Jin et al. (2017) and Ma and Chen (2020) performed systematic classifications and simulations of residential areas in Tianjin, China respectively; their findings highlighted significant variations in wind environments across different layout patterns and identified key morphological factors such as frontal area density and mean building height [17,18]. More practice-oriented, Zhang and Zhang (2021) identified appropriate building arrangements for cold-climate cities based on their findings in Shenyang [19]. Recently, Feng et al. (2022) integrated UAV-based field measurements with numerical simulations to extend the research scope into three-dimensional vertical space, identifying building height variation as the most critical factor influencing wind speed ratios across different elevations [20]. Collectively, this research domain has matured from quantitative analysis of singular morphological indicators to multi-factorial, multi-scale systemic evaluations. Yet, a significant research gap persists regarding the correlation between spatial layout configurations and potential cooling efficacy under conditions of constant development intensity.

Focusing on the tropical island city, this study investigates the impacts of building quantity and spatial enclosure forms on the pedestrian-level wind environment and potential cooling efficacy. The analysis is based on typical summer and winter wind characteristics and specifically examines commercial plots under the constraint of constant development intensity. This study constructs a Pedestrian-level Cooling Performance Index (PLCPI) by employing a combined weighting method that integrates the Analytic Hierarchy Process (AHP) and the Entropy Weight Method (EWM), thereby enabling a quantitative comparison and ranking of the cooling performance of various layout configurations. The primary contributions of this study are twofold: First, it proposes a novel dual-season adaptive evaluation framework that balances summer cooling requirements with winter wind environment control, thereby filling a regulatory gap in quantitative wind environment research for commercial plots in tropical regions. Second, it reveals a relationship between building quantity and cooling performance under the constraint of constant development intensity, identifying optimal and suboptimal layout forms to provide robust decision support for the meticulous design of urban commercial plots.

2. Study Design

2.1. Research Precondition and Research Framework

Drawing on the existing literature and the central aims of this study, this paper establishes its foundational preconditions and overall research framework (For details, see Figure 1). Prior work offers two lines of evidence supporting a positive correlation between wind speed—and its amplification factor—and pedestrian-level cooling. Direct evidence comes from Feng et al. (2022), Kubota et al. (2008), and Li et al. (2012), who, through field measurements, wind tunnel tests, and numerical simulations, have quantitatively linked building morphology to pedestrian-level wind speed ratios [14,15,20]. Indirect evidence is provided by Jin et al. (2017) and Ma and Chen (2020), who identified building density, frontal area density, and mean building height as key morphological determinants of the pedestrian wind field [17,18]. These findings implicitly validate the mechanism by which building layout regulates thermal comfort through its influence on wind speed. Collectively, the evidence indicates that higher pedestrian-level wind speeds enhance convective heat exchange at the body surface, thereby producing a cooling effect. Accordingly, the operating precondition of this study is that wind speed and its amplification factor are positively correlated with cooling performance at the standard pedestrian height of 1.5 meters.

 doi:10.20944/preprints202605.1065.v1

On this basis, the study turns to an unexplored context—commercial plots in tropical regions. Under a fixed development intensity, it systematically investigates how building count (one to four units) and spatial enclosure form shape the pedestrian-level wind environment and its attendant cooling efficacy. To enable a quantitative comparison among configurations, we introduce the PLCPI. This composite index integrates summer and winter wind speeds and amplification factors through a linear weighted sum (Figure 1). The weights are determined by a hybrid approach that combines the AHP with the EWM [21,22]. This approach preserves the subjective judgment prioritizing summer cooling in tropical island cities while utilizing data dispersion to calibrate the weights, thereby ensuring scientific rigor and rationality.Wind environment simulations encompassing 65 layout scenarios—varying building counts and enclosure types—were performed using the Vent2026 software (Version 20260303(SP1)).

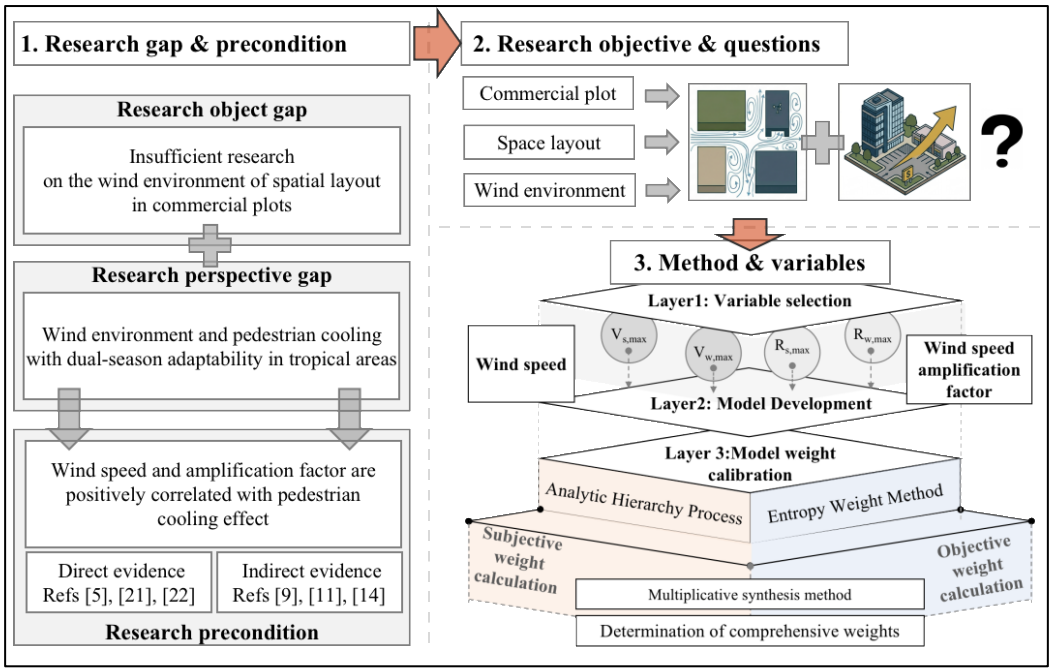

Figure 1. Research framework.

2.2. Case Study Selection

Haikou sits at the northern edge of Hainan Island, China's southernmost province, on the low-latitude tropical fringe. The city experiences a classic tropical maritime monsoon climate, marked by year-round heat and abundant rainfall, with long, intensely hot, and humid summers. The annual mean temperature hovers between 23 °C to 28 °C, yielding generally poor outdoor thermal comfort [23]. These hygrothermal conditions create a pressing demand for ventilation-driven cooling in outdoor spaces, making Haikou an ideal setting in which to examine how building layout can harness wind for thermal relief.

As a tropical island city undergoing accelerated urbanization, Haikou has seen sustained increases in the development intensity of its commercial plots. Under such land constraints, how to improve the outdoor wind environment through refined building layout has become a tangible challenge for local urban design and planning practice. Choosing Haikou as the case study provides a realistic climatic context and a validation setting for the PLCPI model proposed in this research; its findings can also serve as a reference for commercial plot development in climatically similar regions. Figure 2 presents the geographical location of Haikou, the immediate surroundings of the site, and the key development parameters. The site is bordered by undeveloped land, so the influence of neighboring buildings on the layout under study can be excluded (Figure 2(b)). The plot has a floor

 doi:10.20944/preprints202605.1065.v1

area ratio of 1.6, a site area of 2,500 m², a building coverage of 40%, and a green space ratio of 40% (Figure 2(c)).

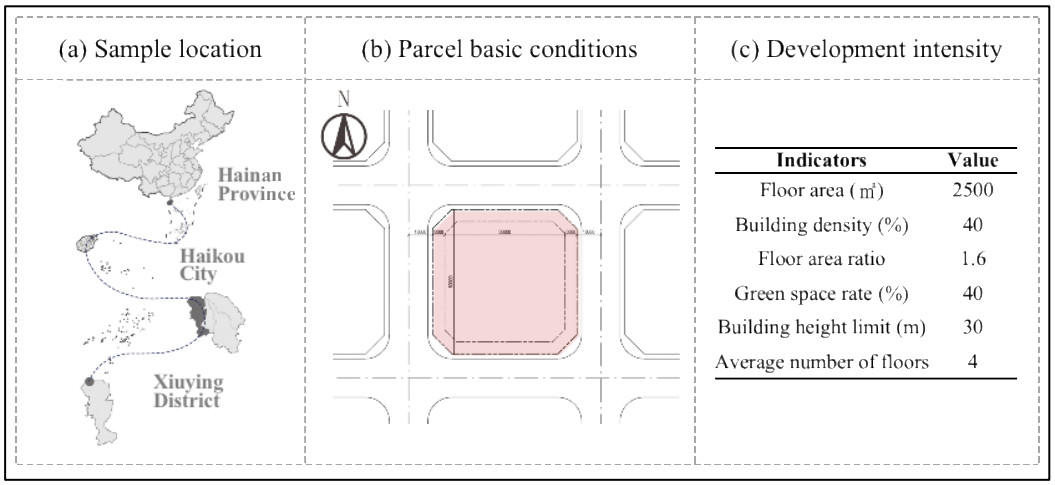

Figure 2. Case study area and development information.

This study operates under the precondition of constant development intensity. That is, key indicators—including building storeys, height, total floor area, building coverage, a minimum fire-separation distance of 6 meters, floor area ratio, and green space ratio—are held fixed. Within these constraints, the permitted total construction area is divided into one to four building blocks, following the standard dimensional conventions of commercial land use (for details, see Figure 3). This subdivision strategy respects the real-world restrictions of high-density urban development while capturing the spatial diversity achievable within a limited repertoire of layout types.

The building configurations on the site are classified into four groups, labeled A through D, with numerical suffixes distinguishing the layout variants within each group (for details, see Figure 3); for instance, B-2 denotes the second layout variant for the two-building condition. The designated layouts also fall into four typological categories: detached layout, row layout, perimeter layout, and courtyard layout. The detailed classification is as follows:

Group A: One building on site, comprising 4 layout variants (A-1 to A-4). All four are detached layouts.

Group B: Two buildings on site, comprising 31 layout variants (B-1 to B-31). Among these, B-1 to B-19 are row layouts, and B-20 to B-31 are perimeter layouts.

Group C: Three buildings on site, comprising 28 layout variants (C-1 to C-28). Among these, C-1 to C-16 are row layouts, and C-17 to C-28 are courtyard layouts.

Group D: Four buildings on site, comprising 2 layout variants (D-1 and D-2). Both are perimeter layouts.

 doi:10.20944/preprints202605.1065.v1

Figure 3. Spatial pattern and layout number.

2.3. Data Collection

In urban microclimate research, the pedestrian-level wind environment is a core determinant of outdoor thermal comfort and cooling efficacy. For tropical island cities, the combination of high

 doi:10.20944/preprints202605.1065.v1

temperatures, high humidity, and intense solar radiation makes natural ventilation the principal means of improving outdoor thermal conditions. During summer, elevated wind speeds around buildings effectively remove heat and moisture from the body surface, markedly improving thermal comfort; conversely, excessive wind speeds in winter can cause wind discomfort, discouraging the use of outdoor spaces. Building cluster design must therefore reconcile summer cooling demand with winter wind comfort, pursuing an integrated optimization that is adaptive to both seasons.

Accordingly, this study adopts building count and spatial enclosure form as independent variables, and selects maximum pedestrian-level wind speeds and their amplification factors in summer and winter as the core evaluation metrics. Through a multi-indicator weighted synthesis, these metrics capture the integrated outdoor cooling performance of alternative spatial layouts under tropical island climatic conditions (For details, see Table 1).

Table 1. Variable definitions.

Variable	Symbol	Effective height(m)	Description
Maximum summer wind speed	Vs,max	1.5	Directly determines the heat dissipation capacity
Maximum summer wind speed amplification factor	Rs,max		Reflects the enhancement of the summer wind by the layout pattern
Maximum winter wind speed	Vw,max		Prevents excessive winter wind speed from compromising comfort
Maximum winter wind speed amplification factor	Rw,max		Reflects the enhancement of the winter wind by the layout pattern

The mesh resolution in wind environment simulation directly affects computational accuracy and efficiency: an overly fine mesh incurs prohibitive computational cost, whereas an overly coarse mesh compromises precision. A rational meshing strategy therefore applies differentiated settings to distinct regions of the computational domain. The refinement scheme adopted in this study is detailed in Table 2. The near-field ground mesh is refined with a subdivision level of 4.000m, while the far-field ground mesh remains coarser at 8.000m. Additionally, informed by the case study context, the power-law exponent for the wind speed gradient profile is set to 0.16, with a gradient wind height of 350m. The standard k-ε turbulence model is employed for the numerical simulation of the flow field.

Table 2. Mesh generation information for wind environment research.

Mesh type	Mesh size (m)	
Regular mesh	Arc division accuracy	0.240
	Maximum mesh size	16.000
	Minimum mesh size	4.000
	Building surface refinement layer thickness	4.000
Ground mesh	Far-field mesh size	8.000
	Near-field mesh size	4.000

According to the wind environment data provided by the Design Code for Heating, Ventilation and Air Conditioning of Civil Buildings (GB50736-2012), the prevailing summer wind in Haikou is southerly at an average speed of 2.700 m/s, while the winter wind is predominantly northeasterly at 3.100 m/s (for details, see Table 3) [24]. All subsequent wind environment calculations and simulation analyses for each layout configuration are based on the baseline values presented in Table 3.

 doi:10.20944/preprints202605.1065.v1

Table 3. Basic wind environment indicators of Haikou, Hainan Province.

Seasons	Wind speed (m/s)	Wind direction	Wind direction angle(°)
Summer	2.700	South	270.00
Winter	3.100	Northeast	22.500

Wind direction angle: counterclockwise positive; east=0°, north=90°, west=180°, south=270°.

3. Model Construction and Weight Calibration

3.1. Model Construction

Computational Fluid Dynamics (CFD) is adopted in this study to resolve the wind field (equation 1). Within the computational domain, the governing equations for mass, momentum, and energy conservation are established and solved using the SIMPLE algorithm as follows:

$$\frac{\partial(\rho\phi)}{\partial t} + div(\rho U\phi) = div\left(\Gamma_\phi grad\phi\right) + S_\phi \quad (1)$$

To quantify the impact of alternative building spatial configurations on pedestrian-level wind speed and cooling efficacy, the PLCPI is constructed. Its formulation follows three principles: summer cooling takes precedence, winter wind environment is controlled, and multiple indicators are synthesized. In tropical island cities, the summer season is prolonged and intensely hot, and outdoor thermal comfort is highly sensitive to wind speed. Accordingly, summer wind speed and its amplification factor are assigned dominant weights in the index. Although the demand for cooling subsides in winter, winter wind speed and its amplification factor are assigned lower weights to avert discomfort from strong winds. This weighting embodies a dual-season adaptive design logic—promoting ventilation in summer while shielding against strong wind in winter. A linear weighted synthesis method integrates four indicators—maximum summer wind speed, summer amplification factor, maximum winter wind speed, and winter amplification factor—into a single composite index that enables quantitative comparison and ranking of cooling performance across layout configurations:

$$PLCPI_i = \alpha_1 V_{s,max} + \alpha_2 R_{s,max} + \alpha_3 V_{w,max} + \alpha_4 R_{w,max} \quad (2)$$

$$\sum \alpha_i = 1, \alpha_1,\alpha_2 > \alpha_3,\alpha_4 \quad (3)$$

In equation (2) and (3), $PLCPI_i$ is the Pedestrian-level Cooling Performance Index for layout type i; $V_{s,max}$ is the maximum wind speed at pedestrian level during summer (m/s); $R_{s,max}$ is the maximum wind speed amplification factor at pedestrian level during summer; $V_{w,max}$ is the maximum wind speed at pedestrian level during winter (m/s); $R_{w,max}$ is the maximum wind speed amplification factor at pedestrian level during winter; α_1 to α_4 are the respective weighting coefficients.

3.2. Calibration of Comprehensive Weight

Determining the weighting coefficients is a critical step in constructing the PLCPI model. To ensure scientific rigor and robustness, this study adopts a combined weighting strategy that couples the AHP with the EWM. This approach integrates professional judgment—which reflects the specific cooling demands of tropical island cities—with the intrinsic information entropy of the simulated data to calibrate the final weights.

Within the AHP 1–9 scale framework, the judgment matrix was logically assigned based on the core climatic characteristic of tropical island cities: strong cooling demand in summer and weak cooling demand in winter. Taking summer wind speed as the reference (assigned a value of 1), it was judged "slightly more important" (value 2) relative to the summer amplification factor due to its direct dominance over ventilation efficiency. Relative to winter wind speed, it was judged "demonstrably more important" (value 6) because summer demand significantly outweighs winter demand. Compared with the winter amplification factor, it was judged "very strongly more

 doi:10.20944/preprints202605.1065.v1

important" (value 7). Based on these pairwise comparisons, the judgment matrix was constructed as shown in Table 4.

Table 4. Judgment matrix.

Variable	$V_{s,max}$	$R_{s,max}$	$V_{w,max}$	$R_{w,max}$
$V_{s,max}$	1.000	2.000	6.000	7.000
$R_{s,max}$	0.500	1.000	3.000	3.500
$V_{w,max}$	0.167	0.333	1.000	1.167
$R_{w,max}$	0.143	0.286	0.857	1.000

Indicator weights were calculated using the geometric mean method, and a consistency check was performed via the maximum eigenvalue. The results yielded a λmax of 4.003, a Consistency Index (CI) of 0.001, and a Consistency Ratio (CR) of 0.001 (<0.100), confirming that the judgment matrix satisfies consistency requirements and that the subjective weights are reasonable. The AHP-derived subjective weights are summarized in Table 5. Concurrently, the Entropy Weight Method was applied for objective weighting, where the weight of each indicator is determined by its degree of variation: greater variation implies greater information content and, consequently, a higher weight.

Table 5. Analytic Hierarchy Process (AHP) results.

Variable	Geometric mean	Subjective weight ($\omega_{i,AHP}$)	λ_{max}	CI	CR
$V_{s,max}$	3.027	0.553	4.003	0.001	0.001
$R_{s,max}$	1.513	0.276			
$V_{w,max}$	0.505	0.092			
$R_{w,max}$	0.432	0.079			

Preliminary data normalization was performed on the dataset. With m layout samples (m=65) and n evaluation indicators (n=4), an original data matrix was established. Because all indicators are positive (higher values indicate better cooling performance), min–max normalization was applied. Based on the quantified sample data, the objective weights for each indicator were calculated and are presented in Table 6. The objective weights reveal that summer indicators—particularly the wind speed amplification factor—exhibit higher data dispersion and carry greater information, which is consistent with empirical observations that diverse layouts markedly influence the summer wind environment.

Table 6. Entropy Weight Method (EWM) results.

Variable	Entropy value (e_j)	Redundancy (d_j)	Objective weight ($\omega_{i,EWM}$)
$V_{s,max}$	0.990	0.010	0.244
$R_{s,max}$	0.991	0.009	0.220
$V_{w,max}$	0.989	0.011	0.268
$R_{w,max}$	0.989	0.011	0.268

Comprehensive weights were derived by integrating the subjective and objective weights using a multiplicative synthesis method (Table 7). In the final weight combination, summer wind speed and its amplification factor receive weights of 0.558 and 0.252, respectively, yielding a combined weight of 0.810. This aligns with the design priority of summer cooling in tropical island cities. The two winter indicators account for a combined weight of only 0.190, ensuring that winter wind conditions remain manageable without distorting the overall cooling assessment. The summer amplification factor carries a lower weight (0.252) than the summer maximum wind speed (0.558). Given that the amplification factor is a dimensionless ratio, it complements the absolute wind speed

 doi:10.20944/preprints202605.1065.v1

within the PLCPI index, and together they provide a robust representation of ventilation and potential cooling efficiency.

Table 7. Results of comprehensive weight calibration.

Variable	Subjective weight	Objective weight	Product	Comprehensive weight
$V_{s,max}$	0.553	0.244	0.123	0.558
$R_{s,max}$	0.276	0.220	0.057	0.252
$V_{w,max}$	0.092	0.268	0.030	0.103
$R_{w,max}$	0.079	0.268	0.019	0.087

4. Results

4.1. Pedestrian-Level Wind Speed

All 65 building spatial layout configurations were imported into the Vent2026 for analysis, yielding pedestrian-level wind speed data for both summer and winter (Figures 4 and 5). Across the 65 configurations, the sample mean of maximum pedestrian-level wind speed in summer is 2.124 m/s (blue dashed line in Figure 4), while the winter counterpart is 2.702 m/s (green dashed line in Figure 5).

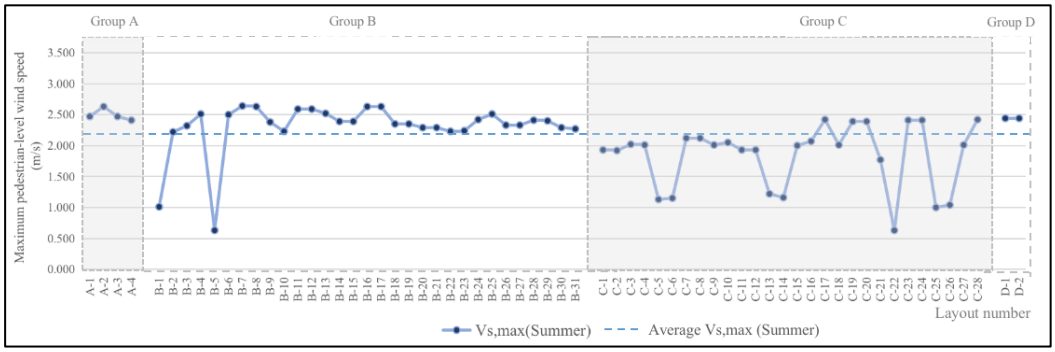

Figure 4. Simulation results of maximum wind speed with base line $V_{s,max}$=2.124.

The sample maximum of summer pedestrian-level wind speed is 2.640 m/s, recorded for layout B-7 (Group B, row layout). Among the 65 configurations, 41 exceed the sample mean in summer. The sample minimum is 0.630 m/s, observed for layout B-5 (Group B, row layout), yielding a range of 2.010 m/s from the maximum. Additionally, layout B-1 (Group B, row layout) registers a notably low summer value of 1.010 m/s, differing from the maximum by 1.630 m/s.

Figure 5 presents the simulated maximum winter pedestrian-level wind speeds for all 65 configurations. The sample maximum reaches 3.100 m/s, attained by layout C-17 (Group C, courtyard layout). Of the 65 configurations, 38 surpass the sample mean in winter. The sample minimum is 1.390 m/s, corresponding to layout C-10 (Group C, courtyard layout).

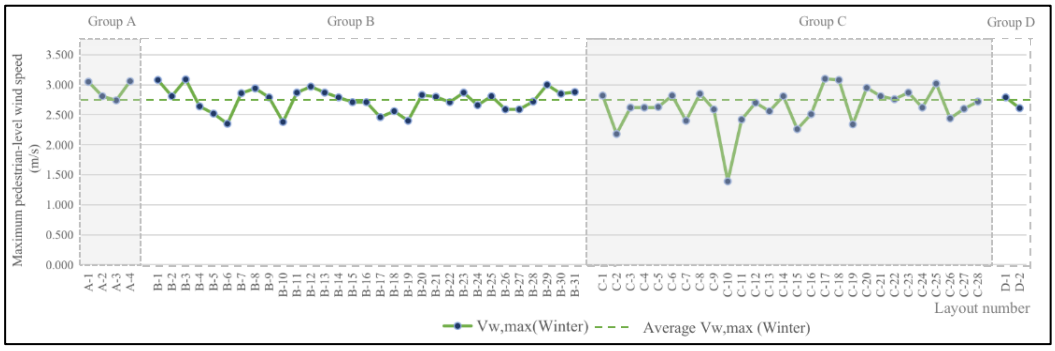

Figure 5. Simulation results of maximum wind speed with base line $V_{w,max}$=2.702.

 doi:10.20944/preprints202605.1065.v1

When examined by group and layout type, Group A's detached layout yields the highest within-group means for both seasons—2.459 m/s in summer and 2.915 m/s in winter—whereas Group C's row layout records the lowest means, 1.798 m/s and 2.511 m/s, respectively (Table 8). Within Group A, only layout A-2 exceeds the group mean in summer (2.630 m/s), while layouts A-1 (3.050 m/s) and A-4 (3.060 m/s) surpass the winter mean.

According to the simulation results summarized in Table 8, the perimeter layout in Group B produces higher within-group mean wind speeds in both summer (2.334 m/s) and winter (2.776 m/s) than the row layout (2.290 m/s and 2.726 m/s, respectively). This indicates that, under the two-building condition, the perimeter layout outperforms the row layout in terms of wind speed and potential pedestrian-level cooling.

Table 8. Sample means of maximum wind speeds in summer and winter.

Group	Number of building units	Layout	$V_{s,max\text{-}mean}$	$V_{w,max\text{-}mean}$
A	1	Detached layout	2.459	2.915
B	2	Row layout	2.290	2.726
		Perimeter layout	2.334	2.776
C	3	Row layout	1.798	2.511
		Courtyard layout	1.908	2.776
D	4	Perimeter layout	2.440	2.700

Similarly, within Group C, the courtyard layout yields higher within-group mean wind speeds (summer: 1.908 m/s; winter: 2.776 m/s) than the row layout (1.798 m/s; 2.511 m/s), suggesting superior ventilation and cooling potential under the three-building condition. Group D, which consists solely of a perimeter layout, records within-group means of 2.440 m/s in summer and 2.700 m/s in winter. Notably, the summer mean trails only that of Group A's detached layout, with a marginal difference of merely 0.019 m/s.

4.2. Pedestrian-Level Wind Speed Amplification Factor

Overall, the sample mean of the maximum summer wind speed amplification factor across all 65 configurations is 1.066, compared with 1.181 in winter, indicating that zones of elevated wind speed in winter offer greater potential cooling benefit than those in summer.

Figure 6 displays the simulated summer amplification factors. The sample maximum of 1.320 is shared by five configurations: A-2 (Group A, detached layout) and B-7, B-8, B-16, and B-17 (Group B, row layout). A total of 41 configurations exceed the summer sample mean.

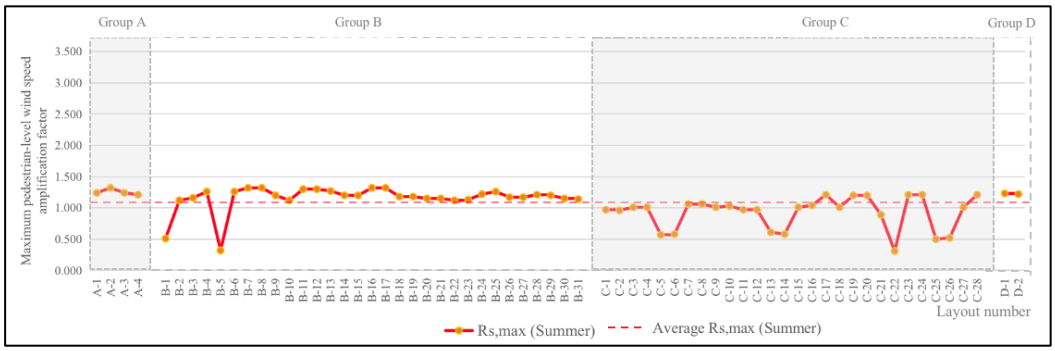

Figure 6. Simulation results of wind speed amplification factor with base line $R_{s,max}$=1.066.

The sample minimum of the summer amplification factor is 0.320, recorded for layout B-5 (Group B, row layout), producing a range of 1.000. Layout B-1 (Group B, row layout) also falls well below the mean at 0.510, a deviation of 0.810.

 doi:10.20944/preprints202605.1065.v1

The winter amplification factor (Figure 7) attains a sample maximum of 1.360 at layout C-17 (Group C, courtyard layout). Of the 65 configurations, 36 surpass the winter sample mean. The sample minimum of 0.610 occurs at layout C-10 (Group C, courtyard layout).

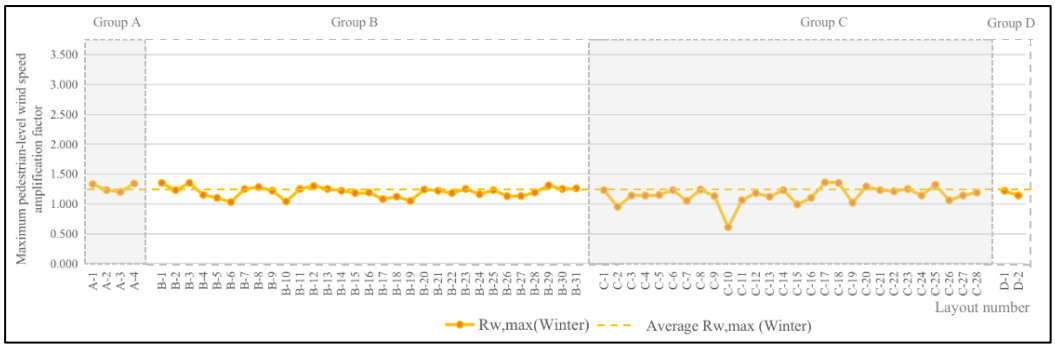

Figure 7. Simulation results of wind speed amplification factor with base line $R_{w,max}$=1.181.

Table 9 presents the within-group means of the amplification factor by season. Group A's detached layout exhibits the highest values (summer:1.253; winter:1.275), while Group C's row layout registers the lowest (summer:0.903; winter:1.097). Within Group A, only layout A-2 surpasses the group mean in summer (1.320), whereas layouts A-1 (1.330) and A-4 (1.340) do so in winter. Based on Table 9, Group B's perimeter layout again outperforms the row layout, with higher within-group mean amplification factors in both summer (1.173vs.1.151) and winter (1.213vs.1.192), further corroborating the enhanced ventilation and cooling potential of the perimeter configuration under the two-building condition.

Table 9. Sample means of maximum wind speed amplification factor in summer and winter.

Group	Number of building units	Layout	$R_{s,max\text{-}mean}$	$R_{w,max\text{-}mean}$
A	1	Detached layout	1.253	1.275
B	2	Row layout	1.151	1.192
		Perimeter layout	1.173	1.213
C	3	Row layout	0.903	1.097
		Courtyard layout	0.957	1.213
D	4	Perimeter layout	1.225	1.180

4.3. Quantification Results of PLCPI

Based on the PLCPI model in equation (2) and the comprehensive weights (Table 7), the indicator data presented in Figures 4 to 7 were substituted to calculate the PLCPI values for all 65 layout configurations. The quantitative results are displayed in Figure 8.

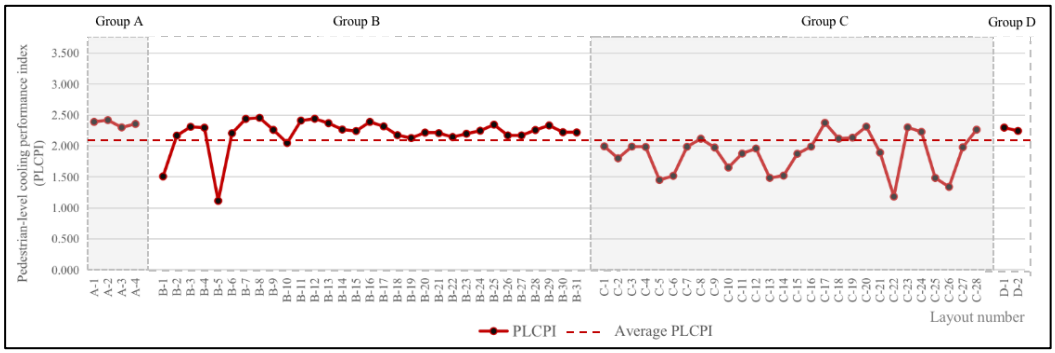

Figure 8. PLCPI value for 65 layouts with base line PLCPI=2.079.

 doi:10.20944/preprints202605.1065.v1

In Figure 8, Group A (one building, four detached layouts) yields PLCPI values between 2.301 and 2.419. Layout A-2 achieves the highest value (2.419), while A-3 records the lowest (2.301). This indicates that even under the single-building condition, differences in building form and orientation measurably affect the pedestrian-level wind environment.

Group B (two buildings, 31 layouts: 19 row and 12 perimeter) exhibits the widest PLCPI range among the four groups, ranging from 1.115 to 2.456. Layout B-8 attains the highest value (2.456)—the overall optimum—whereas B-5 registers the lowest (1.115), the poorest performance. The within-group range of 1.341 underscores that, under the two-building condition, the spatial enclosure form directly governs ventilation efficiency and exerts a decisive influence on cooling performance.

Group C (three buildings, 28 layouts: 16 row and 12 courtyard) produces PLCPI values between 1.184 and 2.375. The maximum occurs at C-17 (2.375) and the minimum at C-22 (1.184). Overall, Group C's PLCPI values are generally low; even its best-performing layout, C-17, is surpassed by numerous configurations in Groups A and B. This suggests that the three-building condition poses greater challenges for ventilation organization, constraining overall cooling performance.

Group D (four buildings, two perimeter layouts) yields PLCPI values of 2.297 (D-1) and 2.244 (D-2), which are closely comparable, with D-1 marginally superior. Despite the limited number of layout variants, both configurations exhibit stable cooling performance with negligible within-group variation.

Averaging the PLCPI values of all 65 layouts by group yields the group-mean PLCPI (Table 10), which reflects the overall cooling performance at different building counts. The results reveal a clear non-linear relationship between building quantity and mean PLCPI. Group A (one building) achieves the highest group mean (2.367). When the count increases to two, the means of Group B's row and perimeter layouts decline to 2.187 and 2.228, respectively. At three buildings, Group C's means drop to the lowest values among all groups (row layout: 1.825; courtyard layout: 1.968). However, at four buildings, Group D's mean rebounds to 2.271—notably higher than Group C and even slightly above Group B. This non-monotonic trend demonstrates that adding buildings does not inevitably degrade cooling performance: the three-building condition marks a performance trough, while the four-building condition outperforms both the two- and three-building scenarios. Under the constraint of constant development intensity, spatial enclosure form and ventilation organization thus emerge as more critical determinants of cooling performance than building count alone.

Table 10. Mean value of PLCPI for four groups.

Group	Number of building units	Layout	$PLCPI_{mean}$
A	1	Detached layout	2.367
B	2	Row layout	2.187
		Perimeter layout	2.228
C	3	Row layout	1.825
		Courtyard layout	1.968
D	4	Perimeter layout	2.271

Group A's PLCPI mean (2.367) is the highest among the four groups, indicating that the fewest buildings achieve the best cooling performance. This advantage stems from the fact that the wind environment around a single building is governed primarily by its own form and orientation, free from inter-building sheltering and interference, and hence simpler to organize and control.

The PLCPI means of Group B's row (2.187) and perimeter (2.228) layouts rank third overall. Although the means are moderate, the extreme within-group variation highlights the high sensitivity of cooling performance to layout configuration under the two-building condition.

Group C's PLCPI means are the lowest among all groups, reflecting the weakest overall cooling performance. This suggests that, under the three-building condition, spatial enclosures readily form semi-enclosed or fully enclosed structures that severely impede natural ventilation in summer.

 doi:10.20944/preprints202605.1065.v1

Group D's PLCPI mean (2.271), derived from perimeter layouts, exhibits a narrow range and high stability due to the limited number of layout variants. This indicates that, with four buildings, the spatial organization converges toward a stable ventilation structure, thereby attaining better average cooling performance than Groups B and C.

4. Discussion

Overall, the relationship between building count and cooling performance is not linear. In this study, Group A (one building) attains the highest mean PLCPI, Group C (three buildings) drops to the lowest, and Group D (four buildings) rebounds noticeably. This non-monotonic trend demonstrates that adding buildings does not necessarily degrade cooling performance; under the tropical climate of Haikou, the three-building configuration represents a distinct trough in both wind environment and cooling efficacy.

A single building holds a clear advantage in cooling performance. The mean PLCPI of Group A markedly exceeds that of the other three groups, indicating that, under constant development intensity, a centralized single building can maximize pedestrian-level ventilation efficiency and is the optimal spatial subdivision strategy for cooling. The three-building layout, by contrast, should be adopted with caution: Group C's mean is significantly lower, and several configurations within the group show poor ventilation and cooling. Interpreted alongside Haikou's prevailing southerly summer wind (2.700m/s) and northeasterly winter wind (3.100 m/s), the reasons for the extreme-performing layouts in each group become clearer.

Figure 9 presents the highest- and lowest-PLCPI configurations in Group A along with their wind environment indicators. A-2 achieves the highest PLCPI (2.419), whereas A-3 records the lowest (2.301). A-2 likely features a well-designed windward face, with its building orientation aligned with the summer southerlies, effectively channeling airflow into pedestrian activity zones. In contrast, A-3 deviates in both orientation and spatial composition, resulting in reduced summer ventilation efficiency. Although no mutual interference occurs between buildings in the single-building condition, the building's own form and orientation still exert a significant influence on the pedestrian-level wind environment.

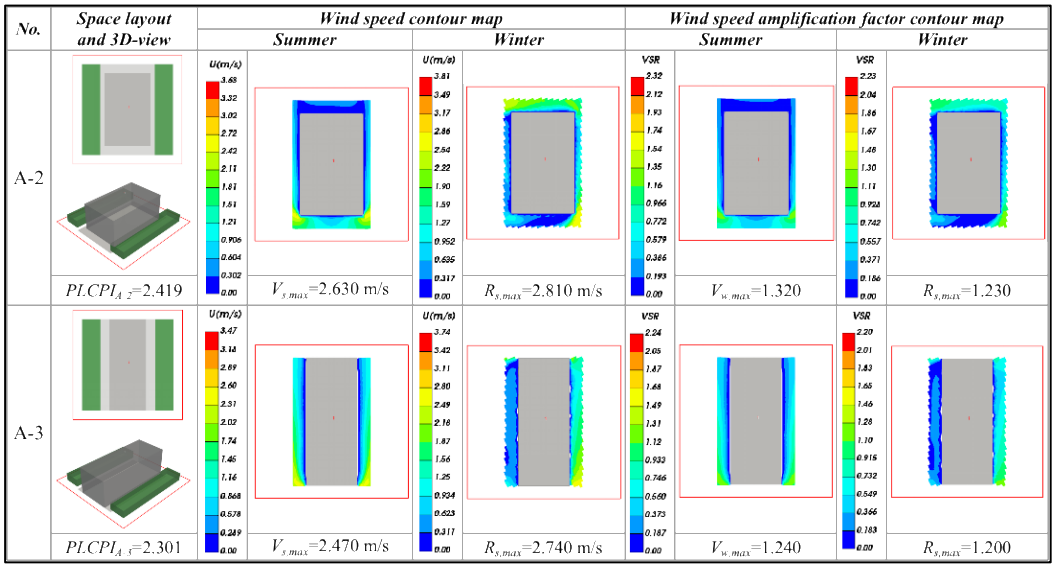

Figure 9. Group A PLCPI extreme value comparison.

In Group B, layout B-8 reaches a PLCPI of 2.456. Its configuration creates an uninterrupted ventilation corridor between the two buildings. With the opening oriented toward the summer southerlies, the layout effectively channels and accelerates airflow across pedestrian areas. Also, the layout appears to avoid generating vortices or strong-wind zones under the winter northeasterlies, thereby limiting the negative impact of winter indicators on the overall index (Figure 10).

 doi:10.20944/preprints202605.1065.v1

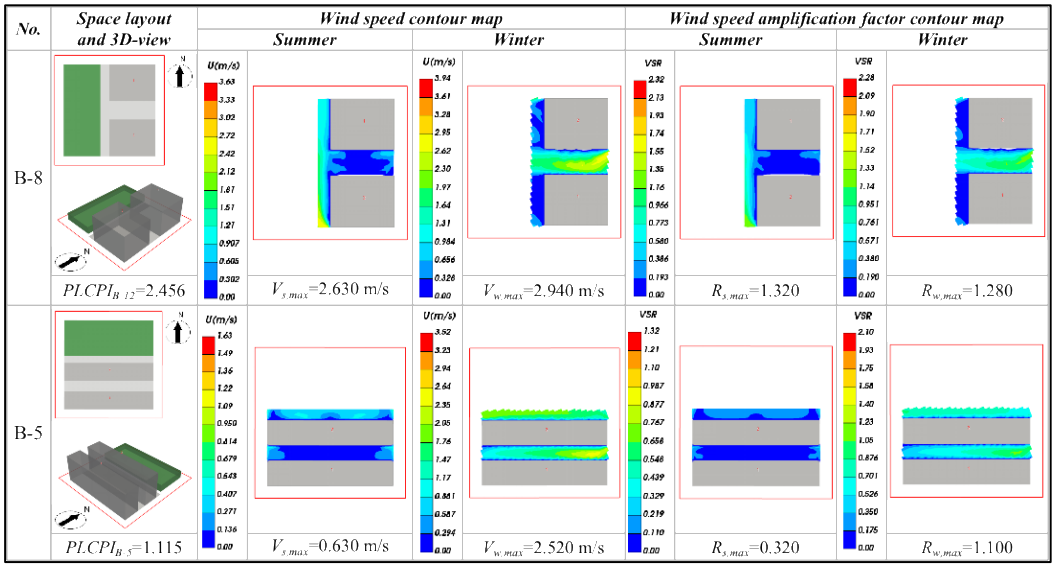

Figure 10. Group B PLCPI extreme value comparison.

Layout B-5, with a PLCPI of only 1.115, most likely forms an enclosed structure whose opening faces away from the summer prevailing wind, preventing southerlies from entering and creating a pronounced wind-shadow zone. The configuration simultaneously intensifies local acceleration of the winter northeasterlies. Given the dominant summer weighting, however, the adverse winter acceleration cannot compensate for the severe shortfall in summer ventilation. Notably, B-8 is the only multi-building layout whose PLCPI surpasses that of the single-building optimum A-2, convincingly demonstrating that, under the two-building condition, precise spatial organization can achieve cooling efficacy superior to that of a centralized single building.

In Group C (Figure 11), layout C-17 attains the highest PLCPI (2.375), while C-22 records the lowest (1.184). C-17 appears to adopt an open arrangement that partially channels airflow into the interior; C-22, however, forms a U-shaped enclosure in which the three buildings fully surround the internal space, and the southern block obstructs the summer southerlies, creating a severe stagnation zone and extremely poor cooling performance. The generally low performance of Group C reflects the difficulty of simultaneously meeting ventilation requirements and spatial enclosure demands with three buildings on a constrained site.

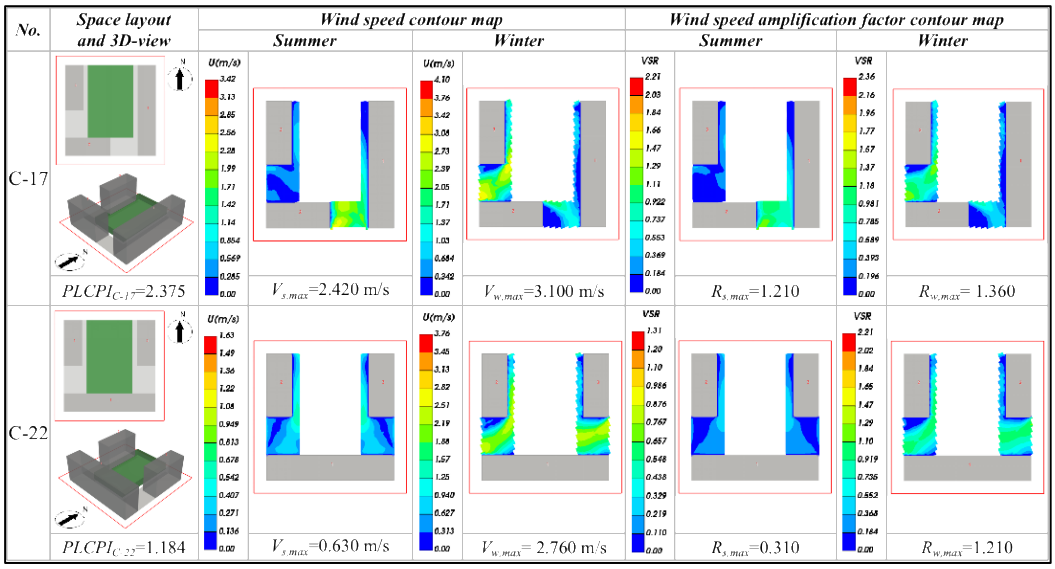

Figure 11. Group C PLCPI extreme value comparison.

 doi:10.20944/preprints202605.1065.v1

In Group D (Figure 12), D-1 and D-2 yield PLCPI values of 2.297 and 2.244, respectively—closely comparable and both at relatively high levels. This group, with four buildings, is configured as a perimeter layout that produces a relatively open, staggered structure, preserving internal spatial integrity while leaving entry channels for the summer southerlies. The high stability of Group D suggests that, when a site necessitates a dispersed arrangement, the four-building mode is more likely to deliver stable cooling performance than the two- or three-building modes.

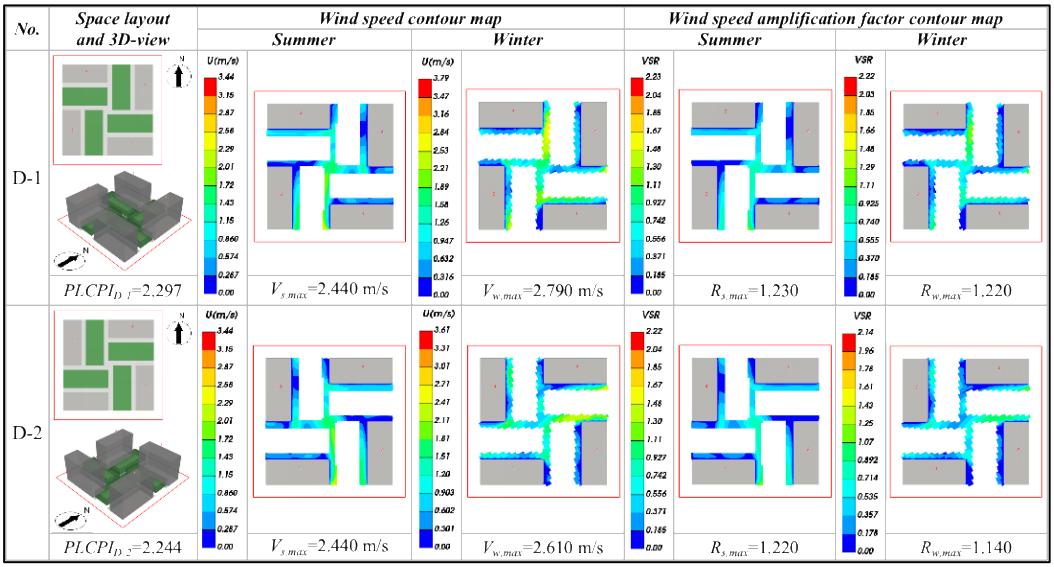

Figure 12. Group D PLCPI extreme value comparison.

Taken together, wind climate—southerly in summer, northeasterly in winter—imposes clear requirements on building layout: designs should prioritize an open windward face toward the summer prevailing wind, create through-ventilation paths, and avoid overly enclosed configurations; at the same time, they must account for winter wind control to avert discomfort from strong winds. Although the single-building layout of Group A performs best on average, the B-8 case demonstrates that a well-designed two-building layout can outperform the single-building optimum, offering a valuable design reference for urban development scenarios that must adopt dispersed building arrangements.

5. Conclusions

Focusing on the tropical island city of Haikou, this study addresses the optimization of building layouts for commercial plots under the constraint of constant development intensity. A Pedestrian-level Cooling Performance Index was constructed, and a combined weighting method integrating the AHP and the EWM was employed to quantitatively evaluate the effects of 65 spatial layout configurations on the pedestrian-level wind environment and cooling efficacy.

The principal findings are as follows:

First, when considering single-season simulation data in isolation, the best summer cooling performance is achieved by layout B-7, a row layout, with a maximum summer wind speed of 2.640 m/s and a maximum summer amplification factor of 1.320. In winter, the best performance is observed for layout C-17, a courtyard layout, where the maximum winter wind speed reaches 3.100 m/s and the amplification factor attains 1.360.

Second, no linear correlation exists between the number of building units and cooling performance. Group A's single-building detached layout yields the highest mean PLCPI of 2.367, representing the optimal spatial subdivision mode. Group C's three-building row layout records the lowest mean PLCPI of 1.825 and should be adopted with caution. Group D's four-building perimeter layout sees the mean PLCPI rebound to 2.271, demonstrating high stability.

 doi:10.20944/preprints202605.1065.v1

Third, when the building count is held constant, the spatial enclosure form is the decisive determinant of cooling performance. Group B (two buildings) exhibits the widest internal PLCPI range: the best layout, B-8, reaches a PLCPI of 2.456, surpassing the single-building optimum A-2 (2.419), while the poorest layout, B-5, records only 1.115. This confirms that, through precise spatial organization, dispersed layouts can outperform even a centralized single building in cooling efficacy.

This study makes two primary contributions. First, it proposes a dual-season adaptive evaluation framework that balances summer cooling with winter wind control, thereby filling a research gap in the quantitative wind environment analysis of commercial plots in tropical regions. Second, it reveals a non-linear relationship between building count and cooling performance under constant development intensity, identifies optimal and suboptimal layout forms suited to tropical island climates, and provides a scientific basis for the meticulous design of urban commercial plots in Haikou.

This study is subject to certain limitations. The experimental design is based on idealized site boundaries and assumes constant development intensity, without accounting for real-world complexities such as surrounding building shading or terrain variations. Future research could incorporate a broader set of realistic urban environmental variables and utilize field measurement data to further validate and calibrate the PLCPI model.

Author Contributions: Conceptualization, Y.C. and J.J.; methodology, J.J.; software, Y.C.; validation, Y.C., J.J. and F.Z.; resources, Y.C.; data curation, Y.C.; writing—original draft preparation, J.J., Y.C; writing—review and editing, Y.C., X.L., F.Z.; visualization, J.J.; supervision, J.J. All authors have read and agreed to the published version of the manuscript.

Funding: This research was funded by the Key Research and Development Project of Hainan Province (No. ZDYF2025GXJS171), Hainan Provincial Natural Science Foundation YouthFund Project (No. 426QN0627), the State Key Laboratory of Tropic Ocean Engineering Materials and Materials Evaluation (No.STOEM99272619).

Data Availability Statement: The data presented in this study are available on request from the corresponding author.

Conflicts of Interest: The authors declare no conflict of interest.

Abbreviations

The following abbreviations are used in this manuscript:

CFD	Computational fluid dynamics
LES	Large Eddy Simulation
PLCPI	Pedestrian-level Cooling Performance Index
AHP	Analytic Hierarchy Process
EWM	Entropy Weight Method

References

1. Liu, Y. S., Tan, Y., Guaralda, M., Degirmenci, K., & Liu, A. (2024). Spatial modelling of urban wind characteristics: Review of contributions to sustainable urban development. Buildings, 14(3), 737.
2. Stathopoulos, T. (1985). Wind environmental conditions around tall buildings with chamfered corners. Journal of Wind Engineering and Industrial Aerodynamics, 21(1), 71-87.
3. Hu, C. H., & Wang, F. (2005). Using a CFD approach for the study of street-level winds in a built-up area. Building and Environment, 40(5), 617-631.
4. Aristodemou, E., Boganegra, L. M., Mottet, L., Pavlidis, D., Constantinou, A., Pain, C., … & ApSimon, H. (2018). How tall buildings affect turbulent air flows and dispersion of pollution within a neighbourhood. Environmental Pollution, 233, 782-796.
5. Lu, M., Song, D., Shi, D., Liu, J., & Wang, L. (2022). Effect of high-rise residential building layout on the spatial vertical wind environment in Harbin, China. Buildings, 12(6), 705.

 doi:10.20944/preprints202605.1065.v1

6. Guo, P. Y., Ding, C. Y., Guo, Z. P., Liu, T., & Liu, T. F. (2022). Coupling CFD simulation and field experiments in summer to prove Feng Shui optimizes courtyard wind environments: A case study of Prince Kung's mansion in Beijing. Buildings, 12(5), 629.
7. Zhao, Y. J., Zhao, K., Lu, J., & Ge, J. (2023). Investigating the temperature distribution of non-enclosed atriums with air infiltration in winter. Building and Environment, 236, 110256.
8. Ngarambe, J., Oh, J. W., Su, M. A., Santamouris, M., & Yun, G. Y. (2021). Influences of wind speed, sky conditions, land use and land cover characteristics on the magnitude of the urban heat island in Seoul: An exploratory analysis. Sustainable Cities and Society, 71, 102953.
9. Davtalab, J., Deyhimi, S. P., Dessi, V., Hafezi, M. R., & Adib, M. (2020). The impact of green space structure on physiological equivalent temperature index in open space. Urban Climate, 31, 100574.
10. Chan, S. Y., & Chau, C. K. (2021). On the study of the effects of microclimate and park and surrounding building configuration on thermal comfort in urban parks. Sustainable Cities and Society, 64, 102512.
11. Deng, J. Y., & Wong, N. H. (2020). Impact of urban canyon geometries on outdoor thermal comfort in central business districts. Sustainable Cities and Society, 53, 101966.
12. Yang, J., Wang, Y., Xiu, C. L., Xiao, X. M., Xia, J. H., & Jin, C. (2020). Optimizing local climate zones to mitigate urban heat island effect in human settlements. Journal of Cleaner Production, 275, 123767.
13. Zeng, P., Zong, C., & Wei, X. (2024). Quantitative analysis and spatial pattern research of built-up environments and surface urban heat island effect in Beijing's main urban area. Journal of Urban Planning and Development, 150(2), 04024006.
14. Kubota, T., Miura, M., Tominaga, Y., & Mochida, A. (2008). Wind tunnel tests on the relationship between building density and pedestrian-level wind velocity: Development of guidelines for realizing acceptable wind environment in residential neighborhoods. Building and Environment, 43(10), 1699-1708.
15. Li, Q., Meng, Q. L., & Zhao, L. H. (2011). Research on wind environment around residential buildings with different planning and design factors. Applied Mechanics and Materials, 121, 725-729.
16. Iqbal, Q. M. Z., & Chan, A. L. S. (2016). Pedestrian level wind environment assessment around group of high-rise cross-shaped buildings: Effect of building shape, separation and orientation. Building and Environment, 101, 45-63.
17. Jin, H., Liu, Z. M., Jin, Y. M., Kang, J., & Liu, J. (2017). The effects of residential area building layout on outdoor wind environment at the pedestrian level in severe cold regions of China. Sustainability, 9(12), 2310.
18. Ma, T., & Chen, T. (2020). Classification and pedestrian-level wind environment assessment among Tianjin's residential area based on numerical simulation. Urban Climate, 34, 100702.
19. Zhang, J. H., & Zhang, X. Q. (2022). Pedestrian-level wind environment assessment of Shenyang's residential areas through numerical simulations. Sustainability, 14(1), 380.
20. Feng, W., Zhen, M., Ding, W., & Zou, Q. S. (2022). Field measurement and numerical simulation of the relationship between the vertical wind environment and building morphology in residential areas in Xi'an, China. Environmental Science and Pollution Research, 29(8), 11663-11674.
21. Saaty, R. W. (1987). The analytic hierarchy process—what it is and how it is used. Mathematical modelling, 9(3-5), 161-176.
22. Shannon, C. E. (1948). A mathematical theory of communication. The Bell system technical journal, 27(3), 379-423.
23. Hu, J.; Lyu, C.; Hou, Y.; Zhu, N.; Liu, K. Research on Summer Indoor Air Conditioning Design Parameters in Haikou City: A Field Study of Indoor Thermal Perception and Comfort. Sustainability 2024, 16, 3864.
24. Ministry of Housing and Urban-Rural Development of the People's Republic of China (MOHURD). Design Code for Heating Ventilation and Air Conditioning of Civil Buildings; GB 50736-2012; China Architecture & Building Press: Beijing, China, 2012.